

SITE EFFECTS IN AN ALLUVIAL VALLEY: A COMPARISON OF ESTIMATES FROM EARTHQUAKE AND MICROTREMOR RECORDS

Miguel RODRÍGUEZ¹, Francisco J CHÁVEZ-GARCÍA² And William R STEPHENSON³

SUMMARY

We present results of the comparison between site effect estimates using different types of data: earthquake and microtremor records. Site effects from earthquake records were analysed using three different techniques that represent the state-of-practice. Microtremor records were analysed using the HVSR technique (horizontal to vertical component spectral ratios). We observed the usual similarities between both sets of results. In a second time, we have investigated the reasons for those similarities. To this end we analysed the nature of wave propagation in microtremor recordings using f-k spectra. Our results suggest a possible explanation of the similarities between estimates of site effects obtained using earthquake records and those obtained using microtremor records.

INTRODUCTION

Site effects play a major role in destructive ground motion. For this reason, many studies have investigated different approaches to estimate site effects, either using modeling of wave propagation or analysis of field data. Observational approaches rely mostly on empirical transfer functions, defined as ratios of spectral amplitudes of earthquake records between a soft soil site and a reference site, assumed free of site effects. Given the difficulty and expense of the seismograph network required to obtain enough records simultaneously at the soft soil sites and at the reference station, alternatives have often been searched. In recent years, there have been many studies that have used microtremor records to estimate the level of amplification caused by soft soil formations (see Bard, 1999, for a very complete review paper). In particular the spectral ratios of horizontal relative to vertical components of motion using microtremor records (HVSR) have known a remarkable popularity. Most studies agree that HVSR allows to determine the resonant frequency of a site with high reliability. However, some authors have cautioned that the level of amplification determined using microtremor records may be very different from that determined using the more standard spectral ratio method. This unsolved problem may be flawing a large number of site effect studies these days. Even a succinct review of the literature points out that HVSR gives very good results in some cases and quite bad results in others. There seem to be a required set of conditions in order to obtain good results, but these conditions have not yet been established.

In this paper we take advantage of a very high quality data set to investigate the similarities and differences between site effect estimates obtained using earthquake records and those obtained using microtremor records. We believe that in order to move forward in the controversy regarding HVSR, we do not only need additional studies showing comparisons of HVSR with standard spectral ratios. We should determine what are the conditions that determine when is it reliable, the estimate of site effects obtained from microtremor records. This research needs to concentrate on the nature of site effects, and on the nature of the wavefield that is contained in the "S-wave window" of earthquake records and in microtremor records. This is the main objective of this paper.

Between 1st August and 12th October, 1995, a dense, temporary array of digital seismographs was deployed in Parkway valley, Wainuiomata, New Zealand. Parkway valley is a small (400 m wide) shallow alluvial valley incised in highly indurated greywacke. The array consisted of 23 autonomous stations, coupled to three-component, 1 Hz seismometers. Four of them were installed on the soft rock (weathered greywacke) surrounding and underlying Parkway basin, while 19 others were installed on the soft sediments filling the valley. The

¹ Instituto de Ingeniería, UNAM, Mexico

² Instituto de Ingeniería, UNAM, Mexico

³ Institute of Geological and Nuclear Sciences, Ltd., New Zealand

average distance between stations was less than 40 m. Figure 1 shows the distribution of the stations. During its operation, the network recorded 64 events at 10 or more stations. In addition to their normal operation, the stations were manually triggered several times to record simultaneously 4 minute windows of ambient vibration. A more detailed account of the experiment and the geology of the valley is given in Chávez-García et al. (1999). In the following lines we will first present a standard analysis of site effects using these data. Second, we investigate the nature of the wavefield present in the microtremor records. This allows us to propose a possible explanation for the similarities and differences between site effect estimates produced with earthquake and microtremor records.

ANALYSIS OF EARTHQUAKE RECORDS

The earthquake records recorded by the temporary array were processed to estimate site effects. These were investigated using three state-of-practice techniques: standard spectral ratios relative to a reference site (SSR); horizontal to vertical spectral ratios (HVSr); and a generalized inversion technique (GIS). The data used were 10 sec windows starting 2 sec before S-wave arrival, extracted using a cosine taper with a length equal to 10% the length of the data window. A detailed account of these techniques, of the processing, and of the results that were obtained is given in Chávez-García et al. (1999). Here we will only recall briefly the main conclusions.

Figure 2 shows for example the observed transfer functions for four stations using the three different techniques. Three of these stations were located on soft soil (06, 16, and 21), while the fourth was located on rock (23). We show the final average estimate using all the records. The agreement between the different estimates is very good, except perhaps the smaller amplitude of the GIS estimate. Similar results are obtained for all the other soft soil sites. The rock sites, as exemplified by station 23, show all a similar behavior, with very small amplification and no consistent peak.

For all the sites on soft soil, a very clear resonance peak can be identified in the empirical transfer functions. We have configured a map of the spatial variation of the frequency of occurrence of this resonant peak for all the soft soil stations. The result is shown in Figure 3. We observe a clear correlation between the isoperiod curves and the shape of Parkway basin, suggesting that the amplification peak is closely related to vertical resonance of shear waves.

ANALYSIS OF MICROTREMOR RECORDS

Microtremor records were obtained at Parkway by manually triggering all the stations simultaneously during 60-sec. We have processed four such windows of microtremor records to estimate site effects, using the HVSr technique. To this end, we divided the data in 10-sec windows (a total of 24). The noise record for each component within each window was processed as follows. The autocorrelation functions was computed and then an average for the 24 windows (each one of 10-sec length) was calculated. A Hamming window was convolved with the average autocorrelation function and finally the power spectrum was computed. The resulting spectra was used to compute horizontal to vertical spectral ratios. The results obtained for the same four stations shown in Figure 2, are shown in Figure 4. This figure allows to compare the estimate of site effects using microtremor records, with the one obtained using earthquake records and the SSR technique, usually considered the more reliable estimate. We observe a very good agreement between both sets of results, remarkable for stations 06 and 16.

Figure 5 shows an overall comparison in terms of resonant frequencies and associated maximum amplification values determined for all the stations. The comparison is made again between HVSr using microtremor records and the values obtained from SSR using earthquake records for the NS component. The result shows that the value of resonant frequency determined using microtremor data is very consistent with that obtained using SSR. The dispersion of microtremor data is larger than that between the two horizontal components analysed using SSR, but it is similar to that observed between SSR and GIS using earthquake data (Chávez-García et al., 1999). The comparison of maximum amplification values determined from microtremor records with those using earthquake data shows a tendency of microtremor records to underestimate the SSR values. This tendency seems to increase with increasing amplitude value. However, the difference between amplification values determined using microtremors and those of the NS component is of the same order of magnitude as that between both horizontal components for SSR and earthquake data. We would not be able to point this observation if we had followed the usual practice of computing averages between both horizontal components.

In a second time, we have investigated the nature of the wavefield that composes microtremor records at Parkway. To this end we have used high resolution f-k spectra (Dudgeon and Mersereau, 1984). The procedure

we used was as follows. We selected a 50-sec length window from each of the four noise recordings made at Parkway, selecting only the stations on soft soil. For each one of those windows we band-pass filtered the noise records with a sequence of 0.3 Hz wide filters. The central frequency of the filters was varied from 0.75 Hz to 3.5 Hz, with 0.1 Hz steps. An f-k spectrum was computed for each filter, and a phase velocity and backazimuth estimated from the coordinates of the maximum peak of the f-k spectrum. Thus, for each of the four original noise recordings, we have an estimate of phase velocity and backazimuth, for each one of the central frequencies of the filters. Finally, we computed an average and a standard deviation for the values of phase velocity and backazimuth from the four determined values for each frequency. The results are shown in Figure 6. At low frequencies (below 1.7 Hz) the scatter is large, but the average phase velocity values do suggest normal dispersion. At higher frequencies, there is a very good agreement between the four estimates, leading to a stable phase velocity estimate from an average direction of 150°. Also in Figure 6 we have plotted theoretical phase velocity dispersion curves for Rayleigh waves, computed from an informed guess of the subsoil layered structure at the center of the valley (see Chávez-García et al., 1999, for a discussion on the velocity model). We observe a very good agreement between the experimental points obtained from the noise measurements, and the theoretical dispersion curves. This strongly suggests that the microtremor records consist predominantly of Rayleigh waves.

DISCUSSION

We observe a very good general agreement between site effects estimated from earthquake data and those estimated from microtremor measurements. The differences between estimates coming from earthquake and microtremor data are smaller than those observed among the three different techniques used to analyse earthquake data. Moreover, Chávez-García et al. (1999) showed that the S-wave window of earthquake records at Parkway was contaminated with Rayleigh waves. Thus, the empirical transfer functions determined using SSR include not only the information of vertical resonance of shear waves, but include information on the properties of Rayleigh waves propagating within the valley. On the other hand, the analysis of microtremor records suggests that they consist mainly of Rayleigh waves. Thus the good agreement we obtain between the empirical transfer functions determined from earthquake or microtremor records is independent of the predominant wavetype.

In order to confirm this idea, we have plotted in Figure 7 a comparison of amplitude transfer functions. We have plotted, as observational results, the average transfer functions obtained from SSR for the NS component for station 16 (at the center of the valley), and the average estimate obtained from noise records using the HVSR technique. In the same figure, we include the theoretical transfer function for vertical SH wave incidence on the layered structure estimated for the center of the valley. Finally, we include the absolute value of the ellipticity at the surface of two Rayleigh wave modes, computed for the same layered structure. The ellipticity curve for the fundamental mode has a discontinuity at 1.5 Hz, and the first higher mode does not exist for frequencies lower than that one. We observe quite a good agreement among all these curves, with the exception of the discontinuity of the ellipticity curves.

This seems to explain two of our observations. The first one is the good agreement between SSR and HVSR using earthquake records. We know that the S-wave window we analysed is contaminated with surface waves, which are absent from the reference station we used. Thus, HVSR would measure the ellipticity of those locally generated Rayleigh waves, while SSR measures both the vertical resonance of shear waves and the contribution of the horizontal components of Rayleigh waves. This would also explain (at least partly) the observed amplification in the vertical component. The second is the good agreement between results using earthquake data and those obtained using noise data. HVSR using noise data measures the ellipticity of Rayleigh waves, which are the predominant propagation mode contained in those records.

CONCLUSIONS

We have presented results of the comparison between site effect estimates using different types of data: earthquake and microtremor records. Site effects from earthquake records were analysed using three different techniques that represent the state-of-practice. Microtremor records were analysed using the HVSR technique (horizontal to vertical component spectral ratios). The difference between earthquake estimates of site effects and microtremor estimates of site effects are smaller than those observed between different techniques applied to earthquake data.

In a second time, we have investigated the reasons for those similarities. To this end we analysed the nature of wave propagation in microtremor recordings using f-k spectra. We observed that Rayleigh waves are the predominant propagation mode contained in microtremor records.

If we recall that the S-wave window of the earthquake records we used is “contaminated” by locally generated surface waves, we explain the similarities between SSR and HVSR (using the same data set) as due to the similarities between a transfer function computed for vertical incidence of SH waves and ellipticity curves of Rayleigh waves computed for the same stratigraphy. This would also explain the good agreement we obtain between transfer functions obtained from SSR and those obtained from HVSR using microtremor records. Thus, according to our results, a condition for the agreement between noise and earthquake data would be that local site effects include a significant part of locally generated surface waves

REFERENCES

Bard, P.-Y. (1999). Microtremor measurements: a tool for site effect estimation?, in K. Irikura, K. Kudo, H. Okada, and T. Sasatani (eds.) *The effects of surface geology on seismic motion 3*, in press.

Chávez-García, F.J., W.R. Stephenson, and M. Rodríguez (1999). Lateral propagation effects observed at Parkway, New Zealand. A case history to compare 1D vs 2D site effects, *Bull. Seism. Soc. Am.* 89,

Dudgeon, D.E. and R.M. Mersereau (1984). *Multidimensional digital signal processing*, Prentice-Hall, Inc., Englewood Cliffs, New Jersey.

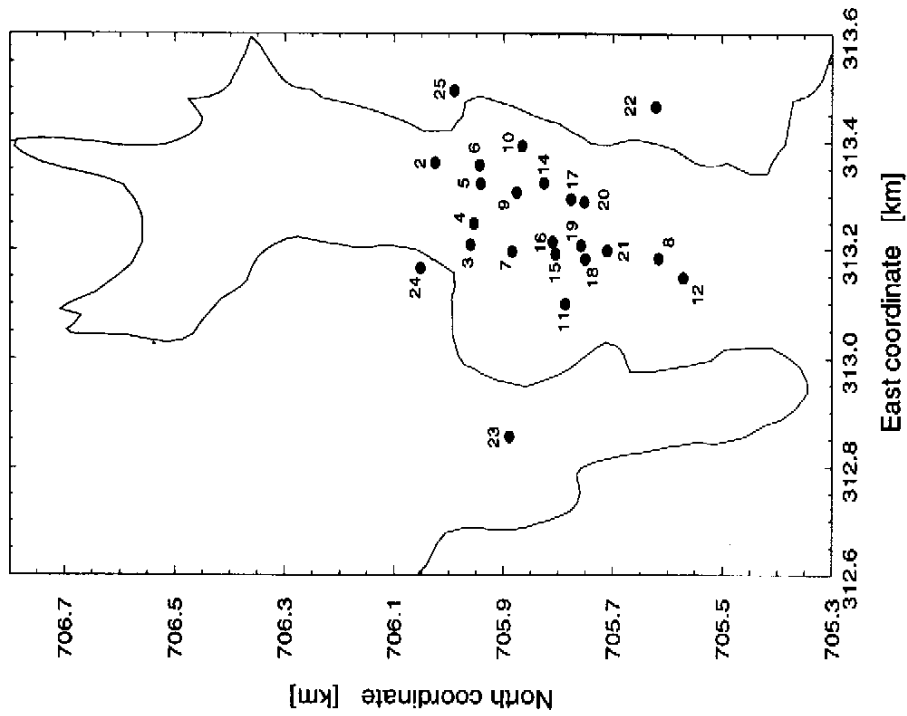


Figure 1. Distribution of the stations in Parkway valley, Wainuiomata, New Zealand. The thin line shows the limit between soft soil sediments and underlying rock.

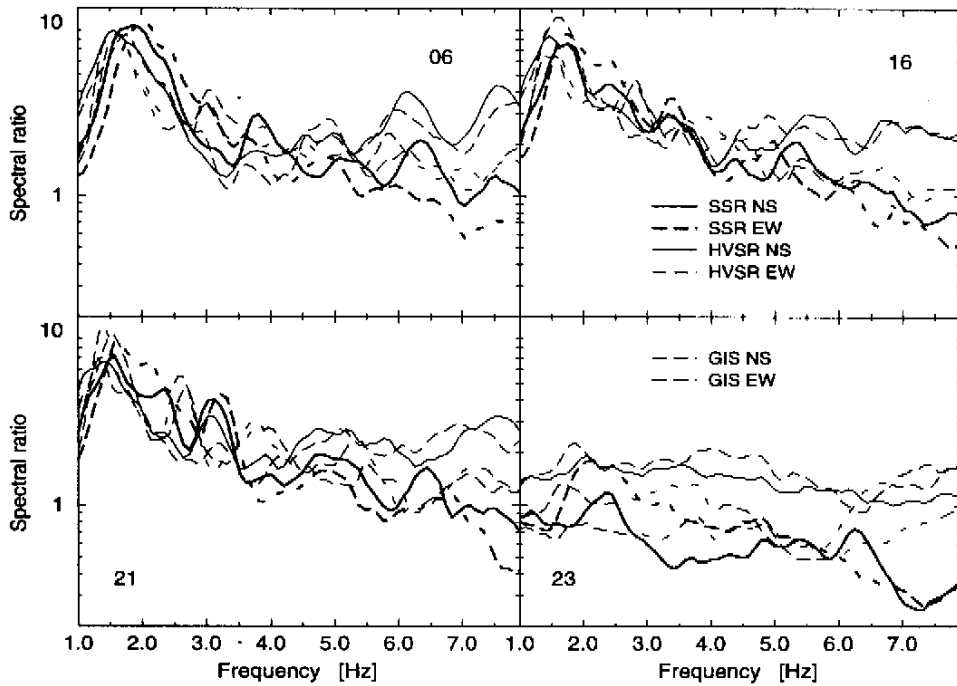


Figure 2. Example of the empirical transfer functions derived from earthquake data. We show the average transfer functions determined for each of the horizontal components and each of the three techniques used: standard spectral ratios (SSR), horizontal to vertical spectral ratios (HVSR), and generalized inversion (GIS). Results are given for three stations on the soft soil sediments (06, 16, and 21) and one rock station (23).

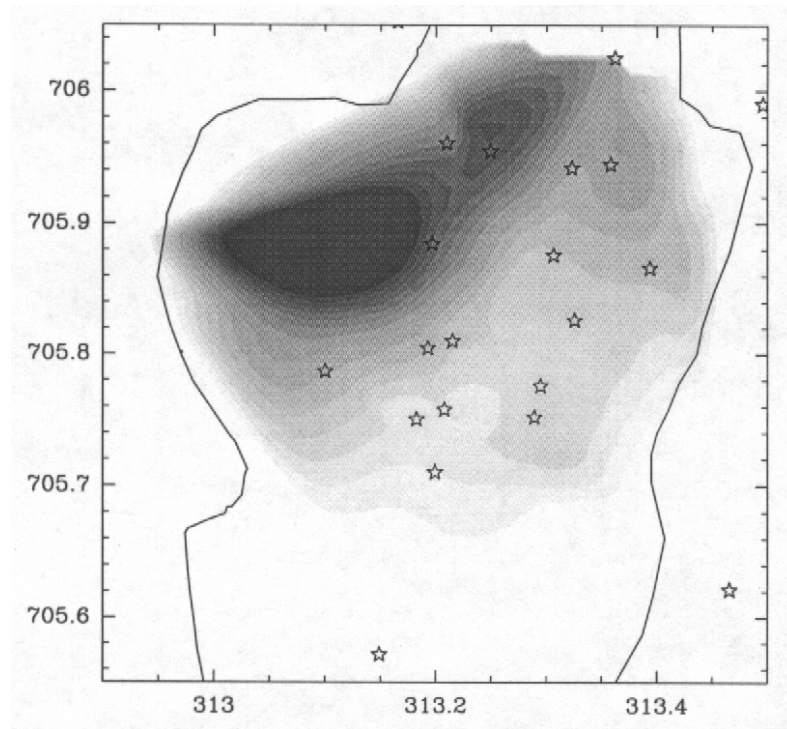


Figure 3. Spatial distribution of the frequency at which the maximum amplification appears in the empirical transfer functions obtained from earthquake records analyzed using the SSR technique for the NS component. The grey scale varies linearly between 1.5 (white) and 2.3 Hz (black). The continuous line shows the contact between soft sediments and underlying bedrock. The stars show the location of the stations. The maximum at coordinates (313.1, 705.9) is an artifact of the interpolation scheme.

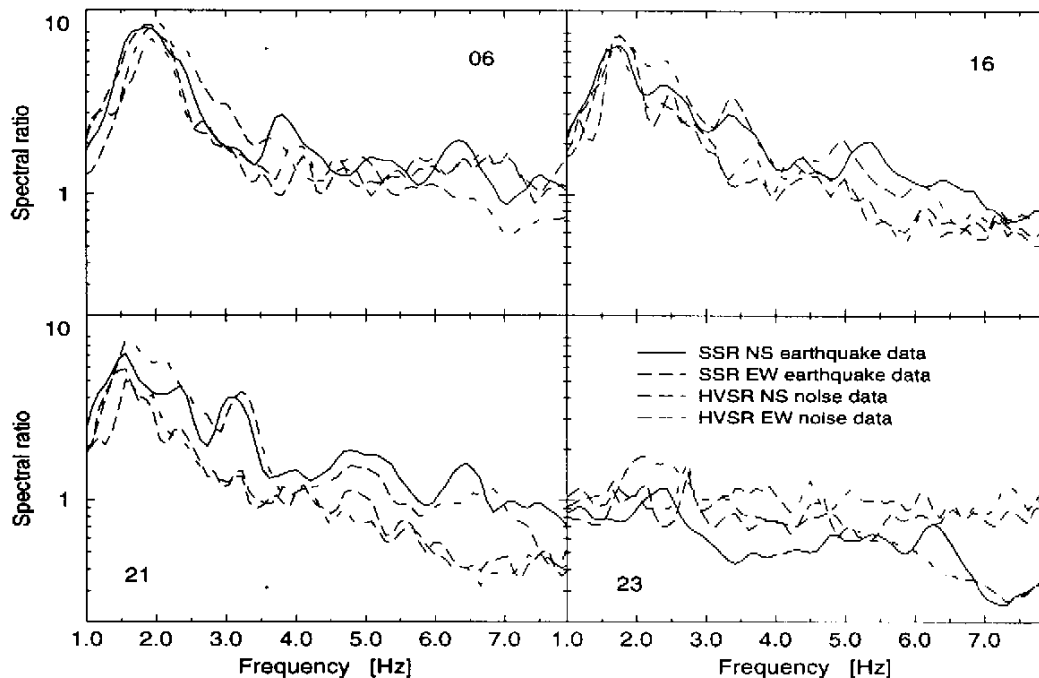


Figure 4. Example of the empirical transfer functions derived from microtremor data. Results are given for three stations on the soft soil sediments (06, 16, and 21) and one rock station (23). We show average transfer functions for both horizontal components determined using the HVSR technique. Results from microtremors are compared with the transfer functions derived from SSR technique for the NS component of earthquake data (solid line in Figure 2). The agreement between microtremor and earthquake data is very good.

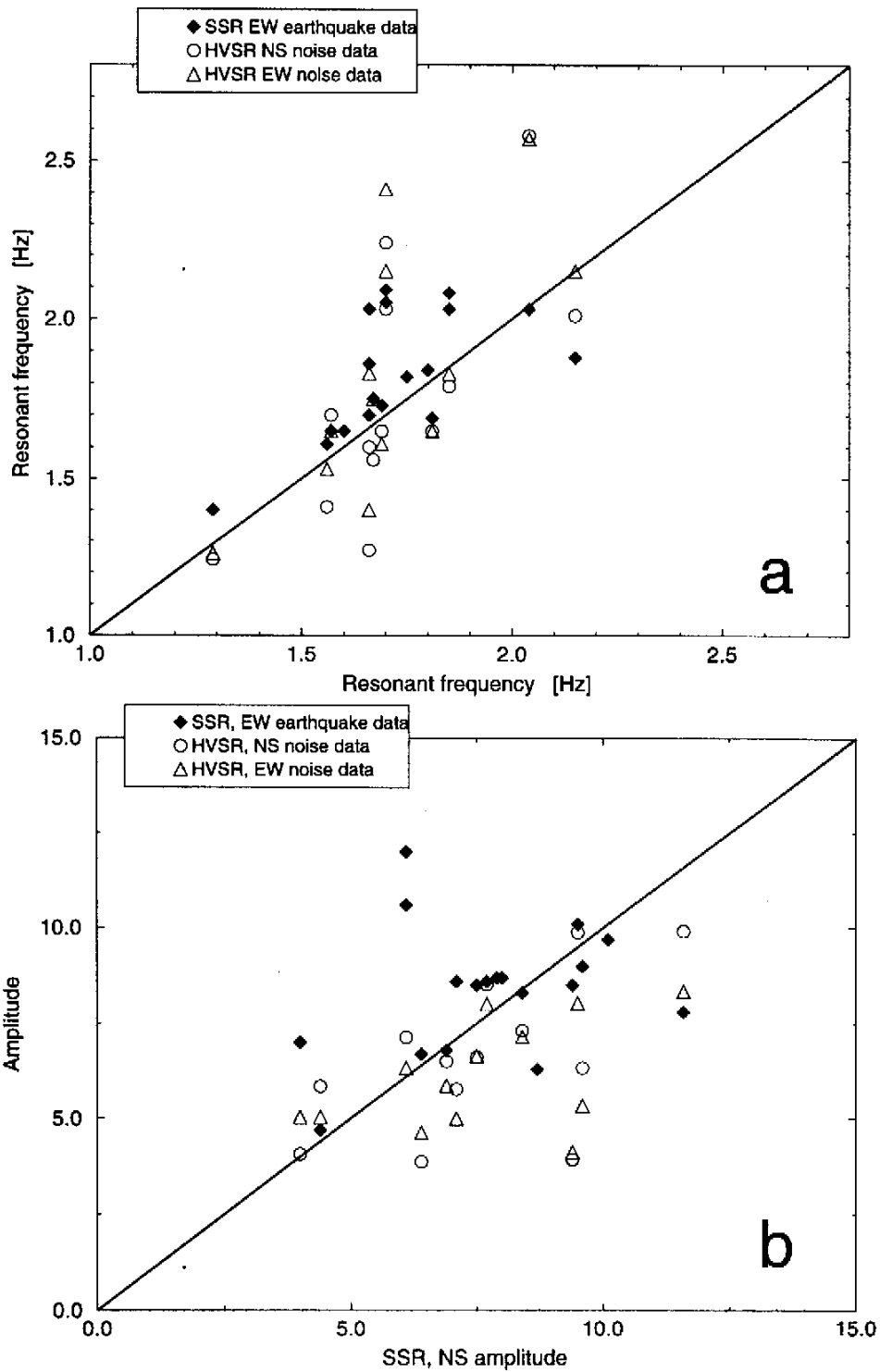


Figure 5. Comparison of resonant frequency (a) and maximum amplification values estimated for the sediment sites in Parkway using earthquake and microtremor data. In the axis of abscissae we have plotted the values obtained from SSR, NS component. In the axis of ordinates we have plotted the values obtained from SSR, EW component (solid symbols) and HVSr, both horizontal components (open symbols). The solid line shows the unit slope.

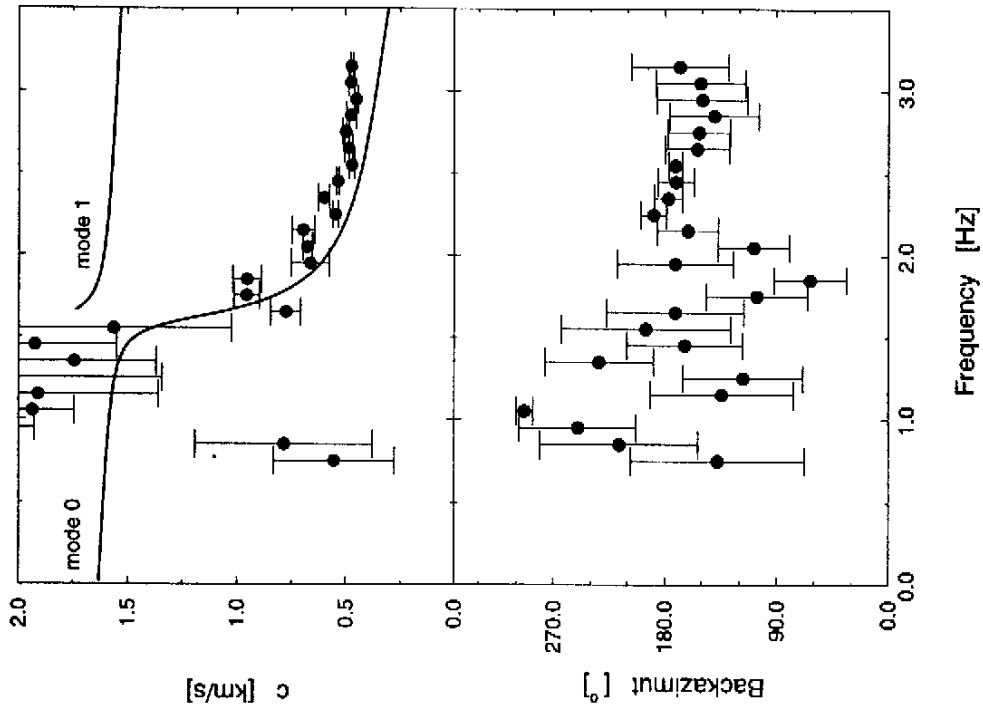


Figure 6. Results of the f - k analysis for the vertical component of the microtremor records. Each solid circle corresponds to the average phase velocity (upper diagram) or backazimuth (lower diagram) determined for a value of central frequency from the four windows analyzed. The bar around each symbol shows the estimated standard deviation. The solid lines show the phase velocity dispersion curves for Rayleigh waves calculated for the stratified structure assumed for the central part of the valley. The fundamental (mode 0) and first higher mode (mode 1) are shown.

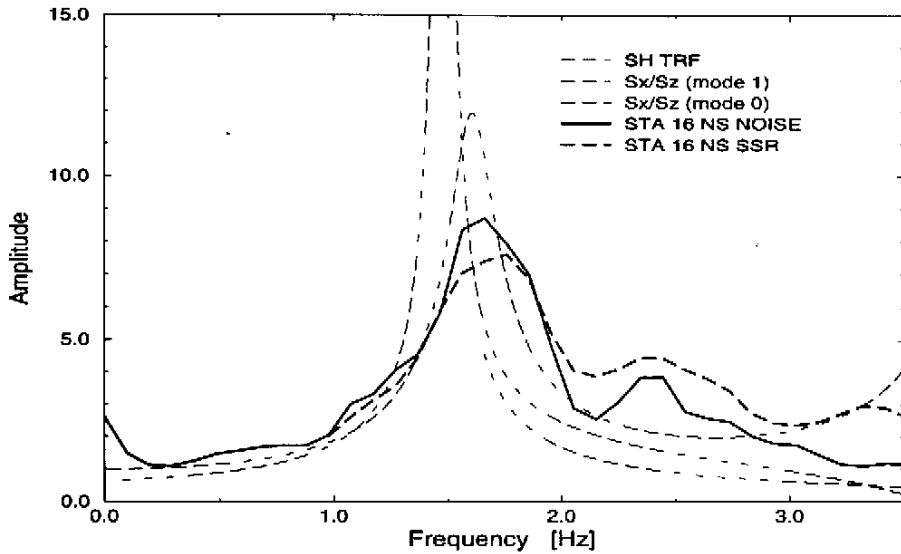


Figure 7. Comparison between numerical and theoretical transfer functions determined for the center of the valley. The solid line shows the average transfer function determined from noise records using the HVSR technique for the NS component. The dotted line shows the final result for the NS component from SSR technique using earthquake data. The dot-dash line (SH TRF) shows the computed transfer function for vertical incidence of SH waves on the layered structure assumed for the center of the valley. Finally, the dashed lines show the ellipticity (S_x/S_z) determined for the fundamental (mode 0) and first higher mode (mode 1) of Rayleigh waves computed for the same layered structure.